J. Embryol. exp. Morph. Vol. 15, 1, pp. 15–37, February 1966
With 2 plates
Printed in Great Britain

The electron microscopy and cytochemistry of oogenesis and the cytochemistry of embryonic development of the prosobranch gastropod *Bembicium nanum* L.

By LYNNE BEDFORD[1]

From the School of Biological Sciences, University of Sydney

INTRODUCTION

While some workers have studied cytochemical localizations during oogenesis in molluscs (e.g. Arvy, 1949, 1950; Bretschneider & Raven, 1951; Collier, 1960; Cowden, 1961; Pasteels & de Harven, 1963), others have examined the ultrastructure of the developing oocyte using the electron microscope (e.g. Rebhun, 1956*a*, *b*, 1961; Worley & Hershenov, 1960; Pasteels & de Harven, 1963). This work has been reviewed by Brachet (1960) and Raven (1961). In the present study of *Bembicium nanum*, both technical procedures have been employed, in an attempt to examine nuclear and nucleolar structure and interrelationships, nucleocytoplasmic relationships and changes in cytoplasmic complexity during oogenesis and vitellogenesis.

Cytochemical localizations and their changing patterns during the embryonic development of molluscs have also been investigated by a number of workers, especially for the embryos of *Limnaea*, *Physa* and *Aplysia*, and reviewed by Raven (1958) and Hess (1962). With the exception of studies on *Limnaea* (Raven, 1958), this work is limited in scope and in no case ventures beyond the trochophore stage. The present work, therefore, also attempts a survey of cytochemical localizations throughout the development of *B. nanum* from the fertilized egg to the hatching veliger.

METHODS

In the histological examination of oogenesis, ovaries were fixed in 5% formol saline or in Bouin, embedded in paraffin (melting point 56 °C), sectioned at 7 μ, stained with Ehrlich's or Heidenhain's haematoxylin and eosin. Living material was also observed by phase-contrast microscopy.

Cytochemical localizations in oogenesis were displayed by the following methods, four replicates of each test being performed:

[1] *Author's address*: School of Biological Sciences, Zoology Building, University of Sydney, New South Wales, Australia.

DNA. Material fixed in Carnoy or 5% formol saline was stained, after sectioning, by the Feulgen reaction (Pearse, 1960). Unhydrolysed sections served as controls.

RNA. Material fixed in Carnoy was stained, after sectioning, with methyl green-pyronin for 30 min (Stein & Gerade, 1950). Control sections were treated with 0·3 M trichloroacetic acid for 5–10 min at 90 °C before staining.

Alkaline phosphatase. Material fixed in 5% formol saline or in acetone at 0 °C for 3 h was mounted as sections on albumen-free slides and stained by the revised metal-salt method of Gomori (Pearse, 1960), using sodium glycerophosphate in the substrate medium. This was omitted in the substrate medium of control sections.

Glycogen. Sections were prepared of material fixed in 5% formol saline, and glycogen was demonstrated by Best's carmine stain (Pearse, 1960). In control sections, glycogen was digested by incubation in saliva at 37 °C for 1 h before staining.

Mucopolysaccharides and glycoproteins. These were demonstrated by the periodic acid-Schiff reaction in sections of material fixed in 5% formol saline (Pearse, 1960).

Iron. Two methods were used in the demonstration of iron, necessitated by the fact that adequate controls are not practicable in either case. The methods, employed on sections fixed in 5% formol saline, were the Prussian Blue test for ferric iron and the Thomas–Lavolloy hydroxyquinoline test (Pearse, 1960). Both methods yielded identical localizations.

In the preparation of ovarian material for electron microscopy, 1 mm blocks of ovarian tissue were fixed in veronal acetate-buffered 2% osmium tetroxide (pH 7·3–7·4) for 2 h at 40 °C or 0 °C. After washing for 2 h in running water, the tissue blocks were dehydrated through an alcohol series, stained in 1% phosphotungstic acid in absolute alcohol for 2 h, rinsed in absolute alcohol, rinsed in xylene for 2 min, then infiltrated for 6 h at room temperature in a standard 'Araldite' mixture and embedded in no. 4 gelatin capsules. The blocks were polymerized at 60 °C for 24 h and sectioned on an L.K.B. ultramicrotome. A Siemens Elmiskop I or II was used for viewing.

Developing embryos were prepared for histological examination by fixation in Smith's formol bichromate or in 5% formol saline, celloidin embedding by the Peterfi method (Pantin, 1948), sectioning at 7μ and staining with Ehrlich's or Heidenhain's haematoxylin and eosin. Cytochemical localizations during embryonic development were displayed by the methods described above.

RESULTS

Oogenesis

The germinal epithelial cells of the ovary, which include the oogonia, are flattened cells with oval, densely staining nuclei lacking nucleoli (Text-fig. 1 A).

The oogonia, after rounding up, undergo repeated mitotic divisions and the daughter cells of these divisions become the oocytes. As each oocyte begins to grow, projecting into the lumen of the ovarian tubule, it becomes covered by a layer of follicle cells derived from the germinal epithelium (Text-fig. 1B). Later

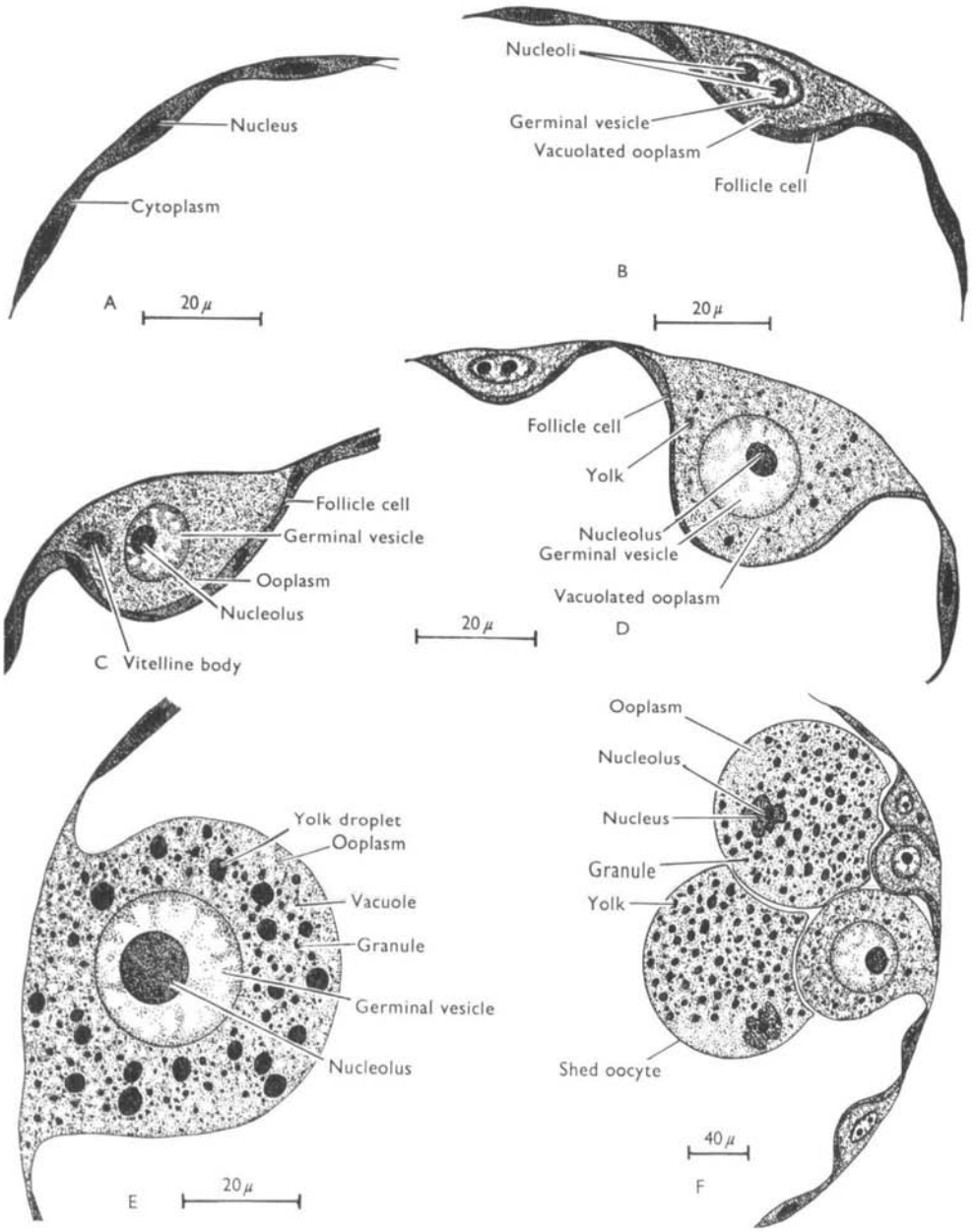

Text-fig. 1. Oogenesis. A, Germinal epithelial cells; B–E, developing oocytes; F, transverse section through the wall of an ovarian tubule showing developing and shed oocytes.

in development of the oocyte, the follicle cells become thinner (Text-fig. 1 D) and finally disappear (Text-fig. 1 E).

The oocyte nucleus. In the early oocyte the nucleus swells into a germinal vesicle (Text-fig. 1 B) and develops two or three nucleoli. The number of nucleoli is then reduced to one (Text-fig. 1 C). Both the germinal vesicle and its nucleolus grow progressively during oogenesis. When the fully grown oocyte is shed into the ovarian lumen, the nucleus and the nueleolus shrink and become densely staining and the surface of the nucleus is thrown into folds (Text-fig. 1 F).

While the germinal vesicle is small, its nucleoplasm is uniformly osmiophobe and the fibrillar loops of lampbrush chromosomes can be seen within it (Plate 1, fig. C). Later in its growth, it becomes filled with granular osmiophobe material and the lampbrush chromosome loops can no longer be detected (Plate 2, fig. A). The nuclear membrane is a typical perforated double membrane in which the pores are lined by annuli and closed by thin membranes. During the early growth of the germinal vesicle, the membranes bulge out into the cytoplasm (Plate 1, fig. A), but after shrinkage of the germinal vesicle in the late oocyte the pore membranes bulge inwards into the nucleoplasm (Plate 2, fig. A).

The nucleolus of the germinal vesicle is granular internally and, prior to vitellogenesis, shows many projections into the nucleoplasm (Plate 1, fig. A). During early oocyte growth, nucleolar budding is prolific. Numerous fragments of nucleolar material are seen in the nucleoplasm and a large amount of the same material accumulates under the nuclear membrane (Plate 1, fig. A; Plate 2, fig. C). However, in the later oocytes, especially after yolk deposition has commenced, nucleolar budding ceases and the amount of nucleolar material lining the inner surface of the nuclear membrane diminishes and finally disappears (Plate 2, fig. A).

Cytochemically, DNA is detectable in the early germinal vesicle, but not after it has enlarged, probably because of dispersal of the lampbrush chromosomes.

Explanation of Plates

All electron micrographs are × 15 000, excepting Plate 1 B, which is × 75 000. All figures are electron micrographs of developing oocytes of *Bembicium nanum.*

Abbreviations: *E.R.*, endoplasmic reticulum; *G*, Golgi apparatus; *G.P.*, granular proteid yolk; *G.V.*, germinal vesicle; *L.*, lipid yolk; *L.P.*, large heterogeneous proteid yolk platelets; *M.*, mitochondrion; *N.*, nucleolus; *N.L.M.*, nucleolar material; *N.M.*, nuclear membrane; *O.V.*, osmiophilic vesicle; *P.*, pore in nuclear membrane; *R.P.*, proteid yolk platelet surrounded by osmiophilic ring; *V.B.*, vitelline body.

Plate 1

Fig. A. Portions of two early oocytes. A vitelline body and lamellae parallel to the nuclear membrane can be seen in the cytoplasm of the upper oocyte. The membrane covering each pore of the nuclear membrane can be seen bulging into the cytoplasm.

Fig. B. Cytoplasm of a late oocyte showing fragments of the endoplasmic reticulum and lipid and proteid yolk.

Fig. C. Early oocyte showing fragmentary endoplasmic reticular lamellae. Yolk-filled cytoplasm of a late oocyte is visible on the right, the vitelline body of an early oocyte on the left.

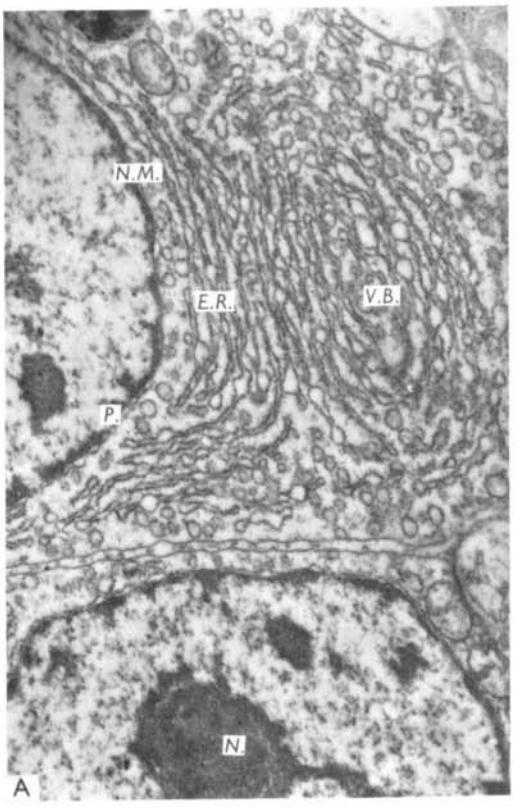
N.M.
E.R.
V.B.
P.
N.
A

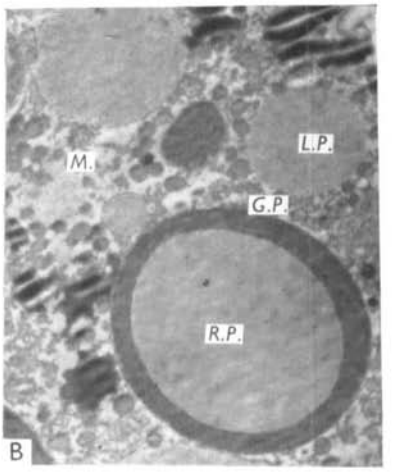
M.
L.P.
G.P.
R.P.
B

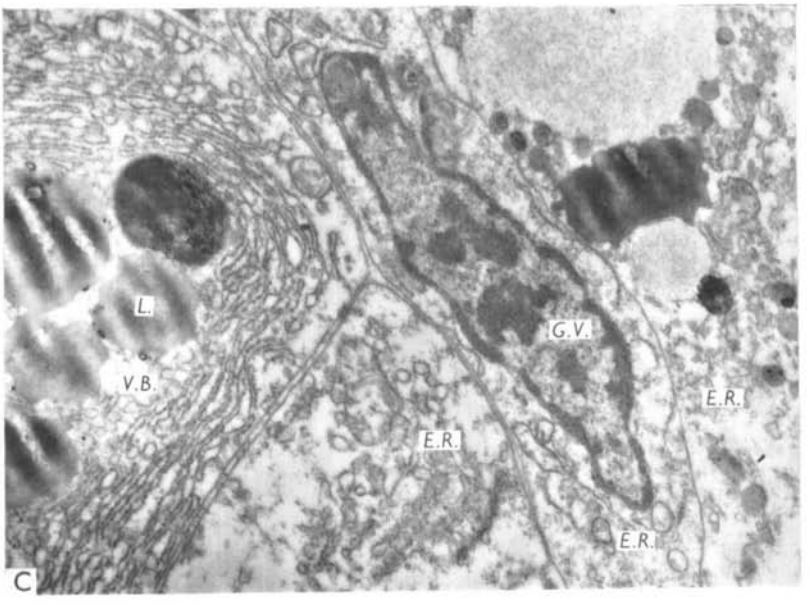
L.
V.B.
G.V.
E.R.
E.R.
E.R.
C

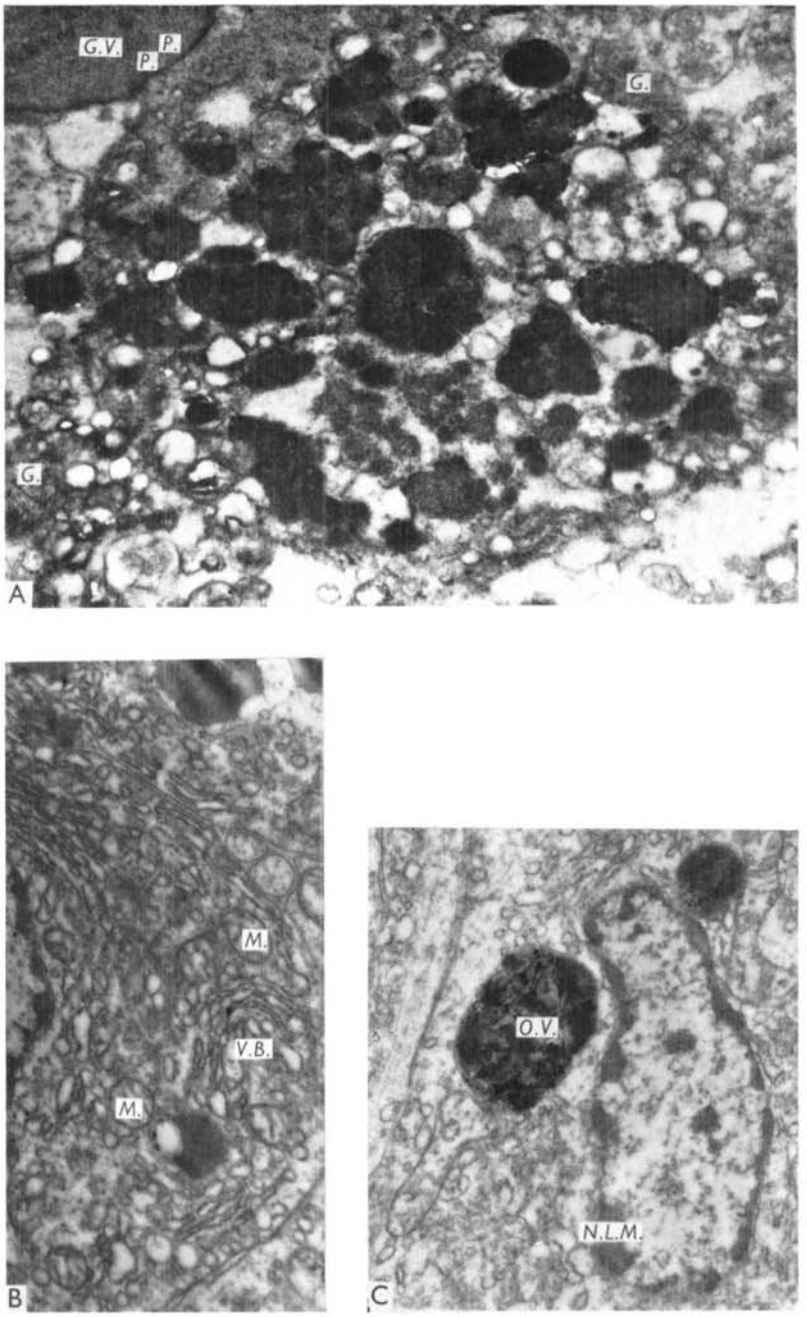

Fig. A. Portion of the cytoplasm of a late oocyte and part of the germinal vesicle. Note the membrane which covers each nuclear pore and which projects into the nuclear plasm. Proteid yolk platelets are found in association with the Golgi apparatus.

Fig. B. Early oocyte showing mitochondria and a vitelline body composed of concentric lamellae.

Fig. C. Early oocyte with a large osmiophilic vesicle to one side of the germinal vesicle.

The nucleoli of the early germinal vesicle are rich in alkaline phosphatase and RNA, and contain small amounts of iron and PAS-positive material. In the single nucleolus of the later germinal vesicle, only small amounts of RNA and alkaline phosphatase persist. Alkaline phosphatase is present in the nucleoplasm throughout oogenesis. These results are summarized in Table 3.

Table 1. *Cleavage times*

Stage	Duration of stage (h)	Hours after oviposition
1-celled stage	5	5
2-celled stage, first cleavage	3	8
4-celled stage, second cleavage	2	10
8-celled stage, third cleavage	3	13
Fourth cleavage	5	18
Fifth and Sixth cleavage	4	22
Successive rapid cleavages to form blastula	8	34
Placula	4	38

The oocyte cytoplasm. Very early in oocyte growth, the cytoplasm contains clumps and strands of 150 Å granules and a few small mitochondria. No Golgi bodies are visible (Plate 1, fig. C). During previtellogenesis, the 150 Å granules increase in number, some being found around endoplasmic vesicles and others along the lamellae of an endoplasmic reticulum which develops more or less parallel to the nuclear membrane. As the oocyte enlarges, the endoplasmic reticulum becomes increasingly well developed, as numerous stacks of parallel lamellae which still lie at first around the germinal vesicle (Plate 1, fig. A), but later become more dispersed (Plate 1, fig. C).

A vitelline body (Plate 2, fig. B), which is composed of mitochondria and granulated endoplasmic lamellae arranged in whorls around a central region of granular cytoplasm, appears during the elaboration of the endoplasmic reticulum. As the oocyte grows, the number of lamellar whorls in the vitelline body increases (Plate 1, fig. A) and one or more lipid droplets appear in the central cytoplasm (Plate 1, fig. C). During this phase of oocyte growth, mitochondria, initially found in the perinuclear region (Plate 2, fig. B), increase in size and number and begin to disperse throughout the oocyte cytoplasm. A similar change is found in the distribution of the Golgi bodies, which are composed of smooth vesicles with osmiophobe centres and osmiophil peripheries, and smaller, uniformly osmiophil, vesicles and lamellae (Plate 2, fig. A).

In the early oocyte, a large vesicle about 1 μ in diameter occurs to one side of the germinal vesicle (Plate 2, fig. C). It is filled with dense osmiophilic material and surrounded by clear cytoplasm, and lies in close association with a large mitochondrion.

Further development of the oocyte is characterized by vitellogenesis, accom-

Table 2. *Embryonic development*

Stage	Duration of stage (d and h)	Time after oviposition (d and h)
Gastrula	12 h	2 d, 2 h
Trochophore—showing little development of foot, mesoderm and shell gland rudiments	1 d, 6 h	3 d, 8 h
Trochophore—showing well developed foot and shell rudiments	1 d, 0 h	4 d, 8 h
Veliger—showing rotation within envelope	2 d, 0 h	6 d, 8 h
Veliger—development till hatching	10 d, 0 h	16 d, 8 h

panied by changes in all cytoplasmic inclusions. The lamellae of the endoplasmic reticulum and the concentric lamellae of the vitelline body become dispersed throughout the oocyte cytoplasm as scattered fragments of stacks of parallel lamellae until, in the late oocyte, no regular arrangement of lamellae is visible (Plate 1, figs. B, C). The mitochondria are disseminated throughout the cytoplasm and appear, in the shed oocyte, to be smaller in size (Plate 1, fig. B). Proteid yolk appears to be primarily deposited in the dispersed Golgi vesicles (Plate 2, fig. A). In the cytoplasm of the late and shed oocyte, numerous Golgi vesicles and lamellae are found in association with the proteid yolk platelets.

Three main types of proteid yolk platelets are found in the cytoplasm of the mature oocyte: (i) large platelets, 1–6μ in diameter, surrounded by a ring of dense osmiophil material (Plate 1, fig. B); (ii) large platelets 0·5–6μ in diameter, com-

Table 3. *Cytochemical localizations during oogenesis*

	Results of cytochemical tests					
Stage	DNA	RNA	Alkaline phosphatase	Iron	PAS-positive	Glycogen
Germinal						
Epithelial cell						
Nucleus	++	−	+	−	−	−
Cytoplasm	−	++	+	−	++	−
Early oocyte						
Germinal vesicle	+	−	+	−	−	−
Nucleoli	−	+++	++	+	+	−
Cytoplasm	−	+++	++	+	++	+
Late oocyte						
Germinal vesicle	−	−	+	−	−	−
Nucleolus	−	+	+	−	−	−
Cytoplasm	−	+	+	++	+++	+++

−, negative reaction to test; +, slightly positive reaction to test; ++, medium positive reaction to test; +++, strongly positive reaction to test.

posed of heterogeneous granular material and bordered by fragmented parts of the Golgi vesicles (Plate 1, fig. B); (iii) smaller, more osmiophilic granules, 0·3–1 μ in diameter, also surrounded by parts of the Golgi elements (Plate 1, fig. B).

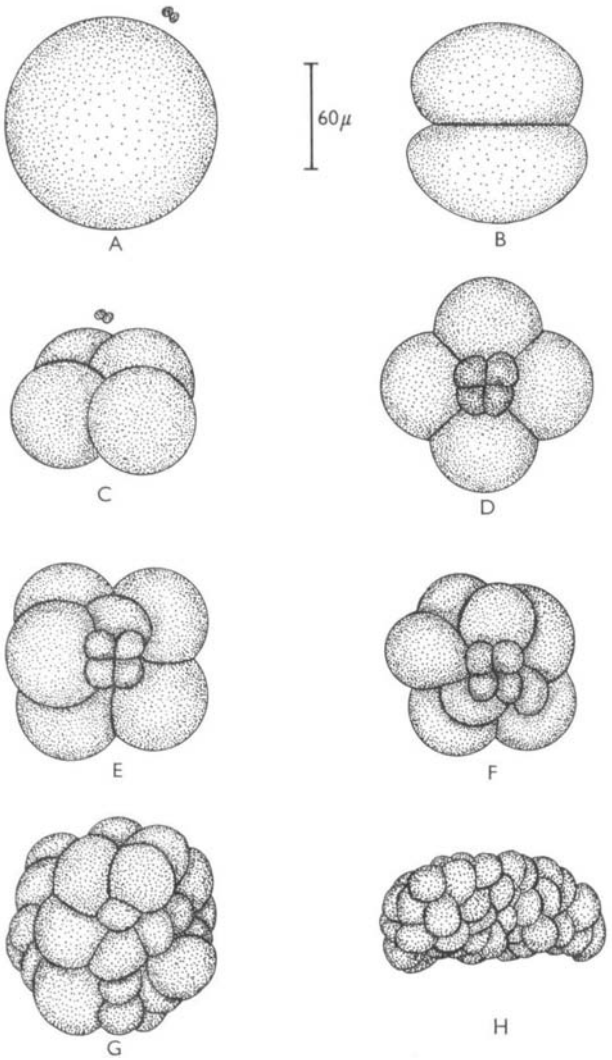

Text-fig. 2. Cleavage. A, 1-cell stage (4 h); B, 2-cell stage (7 h); C, 4-cell stage (9 h); D, 8-cell stage from animal pole (12 h); E, 10-cell stage from animal pole (15 h); F, 12-cell stage from animal pole (18 h); G, blastula from the vegetative pole (30 h); H, placula (38 h).

Cytochemically (Table 3), the oocyte cytoplasm prior to vitellogenesis is rich in RNA, alkaline phosphatase and PAS-positive material. After vitellogenesis, large amounts of PAS-positive material, glycogen, iron and alkaline phosphatase are found associated with the yolk, but the amount of detectable RNA in the cytoplasm has markedly decreased.

Embryonic development

Anderson (1961) briefly described the spawn of *B. nanum* and external features of development of the embryo within the envelope from the trochophore to the hatching veliger.

The fertilized egg. The fertilized egg (Text-fig. 2A) is spherical, opaque, cream in colour, and 120μ in diameter. The proteid and lipid yolk occupies most of the cell contents, but hyaline cytoplasm appears around the nucleus, at the animal pole of the cell and in the cortical region.

Table 4. *Cytochemical localizations following fertilization and during cleavage*

	Results of cytochemical tests					
Stage	DNA	RNA	Alkaline phosphatase	Iron	PAS-positive	Glycogen
Fertilized egg						
Zygote nucleus	++	−	−	−	−	−
Cytoplasm:						
Cortical	−	+	−	++	+	+
Perinuclear	−	++	−	−	+	+
Vegetal	−	−	+	++	+++	+++
Cleavage						
Early cleavage						
Nuclei: mitosis	+	−	−	−	−	−
Nuclei: interphase	−	−	−	−	−	−
Cytoplasm	−	++	+	++	+++	+++
Micromere						
Nucleus	++	−	+	−	−	−
Nucleolus	−	++	−	−	−	−
Cytoplasm	−	++	+	+	+	+
Macromere						
Nucleus	++	−	+	−	−	−
Nucleolus	−	+	−	−	−	−
Cytoplasm	−	+	++	++	++	++

Notation as for Table 3.

The zygote nucleus, situated at the animal pole of the egg, shows a strong positive reaction for DNA. A slight animal-vegetal cytoplasmic gradient is found in the distribution of iron, alkaline phosphatase, PAS-positive material and glycogen, all of which are associated with the yolk. Associated with this animal-vegetal gradient is a barely detectable radial gradient in the distribution of RNA and iron. Positive reactions for RNA are found in the cortical and perinuclear areas, while those for iron, apart from those associated with the yolk, are found in the cortex (Table 4).

Cleavage. Cleavage is of the usual total, spiral pattern (Text-fig. 2). Cleavage times are shown in Table 1. The equal first and second cleavage divisions (Text-fig. 2B, C) are followed by a series of unequal divisions, which produce the micromere quartettes (Text-fig. 2D–F). In the late blastula (Text-fig. 3A), teloblastic mesoderm cells are found in the vegetal region on both sides of the small blastocoel. Following the completion of cleavage, the animal and vegetal surfaces of the blastula flatten, so that the blastula transforms into a placula (Text-fig. 2H).

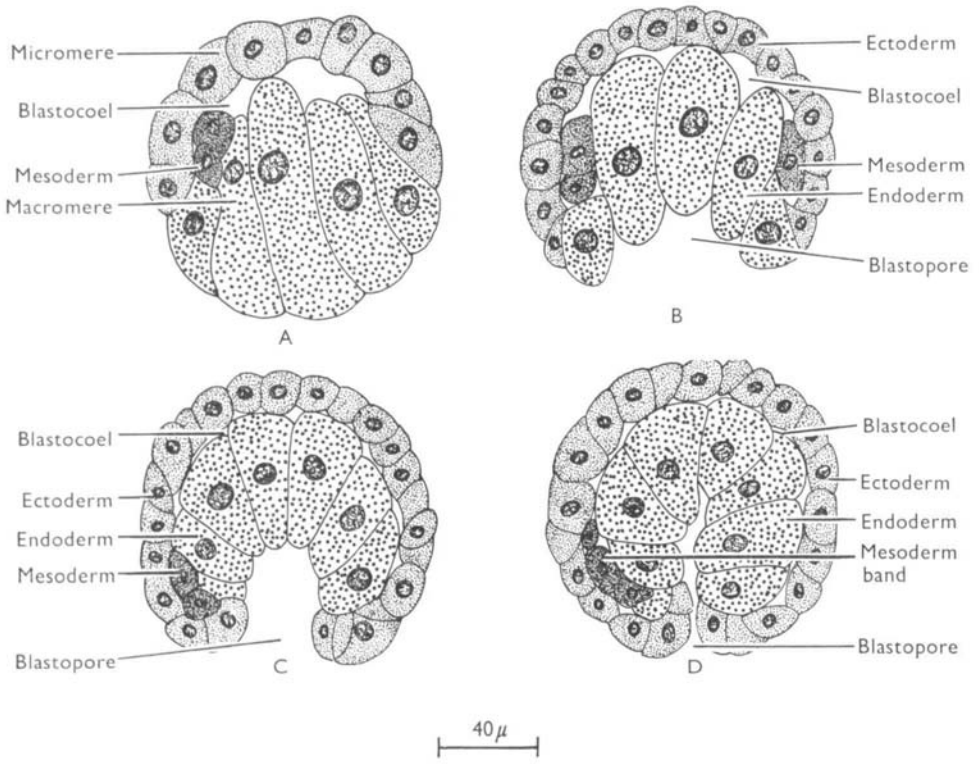

Text-fig. 3. Blastula and gastrulation. A, Vertical section through the blastula (30 h); B, vertical section through the early gastrula (40 h); C, vertical section through later gastrula (44 h); D, vertical section through the late gastrula (48 h).

Apart from an increase in cytoplasmic RNA, the cytochemical distributions in the daughter cells of the early cleavage divisions parallel those of the fertilized egg, but a more definite animal-vegetal gradient is established later in cleavage, due to the association of iron, alkaline phosphatase, PAS-positive material and glycogen with the yolk, most of which is restricted to the macromeres. The micromeres become rich in cytoplasmic and nucleolar RNA, while their nuclei are strongly positive for DNA and slightly positive for alkaline phosphatase. Throughout cleavage, iron is found along the cleavage furrows (Tables 4 and 5).

Gastrulation. The timing of development of the embryo from the onset of

gastrulation to the hatching of the veliger is shown in Table 2. These times are similar to those recorded by Anderson (1961). Soon after formation of the placula, gastrulation commences by invagination of the macromeres at the vegetal pole (Text-fig. 3B) and epibolic growth of the micromeres over the macromeres (Text-fig. 3D). The mesoderm cells (Text-fig. 3B), which lie on both sides in the blastocoel between the ectoderm and endoderm, divide to form mesoderm bands about four cells long (Text-fig. 3D). In the late gastrula and early trochophore (Text-fig. 4A) these compact bands are no longer visible.

Table 5. *Cytochemical localizations in the blastula and gastrula*

	Results of cytochemical tests					
Stage	DNA	RNA	Alkaline phosphatase	Iron	PAS-positive	Glycogen
Blastula						
Ectoderm						
Nucleus	++	−	+	−	−	−
Nucleolus	−	++	−	−	−	−
Cytoplasm	−	++	+	+	+	+
Endoderm						
Nucleus	+	−	−	−	−	−
Nucleolus	−	+	−	−	−	−
Cytoplasm	−	+	++	++	++	++
Gastrula						
Ectoderm						
Nucleus	++	−	+	−	−	−
Nucleolus	−	++	−	−	−	−
Cytoplasm	−	++	+	+	+	+
Endoderm						
Nucleus	+	−	−	−	−	−
Nucleolus	−	+	−	−	−	−
Cytoplasm	−	+	++	++	++	++
Mesoderm						
Nucleus	++	−	+	−	−	−
Cytoplasm	−	++	−	−	−	−

Notation as for Table 3.

During gastrulation, both the ectoderm and the mesoderm cells remain strongly positive for DNA and RNA and contain only small amounts of iron, alkaline phosphatase, PAS-positive material and glycogen. The endoderm cells, in contrast, are only slightly DNA and RNA positive and are rich in iron, alkaline phosphatase, PAS-positive material and glycogen (Table 5).

The trochophore. In the trochophore, the ectodermal prototroch cells remain unciliated and little differentiated. The mesoderm cells become mesenchymatous and some proliferation of mesoderm occurs, especially in the region of the

developing velum and the foot, an outgrowth of ventral ectoderm behind the mouth (Text-fig. 4B). At this stage, the shell gland (Text-fig. 4B) first appears postero-laterally as a local thickening in the ectoderm. Its cells, while in close contact with the endoderm, invaginate (Text-fig. 4B), evaginate, flatten and then begin secretion of the shell (Text-fig. 4C).

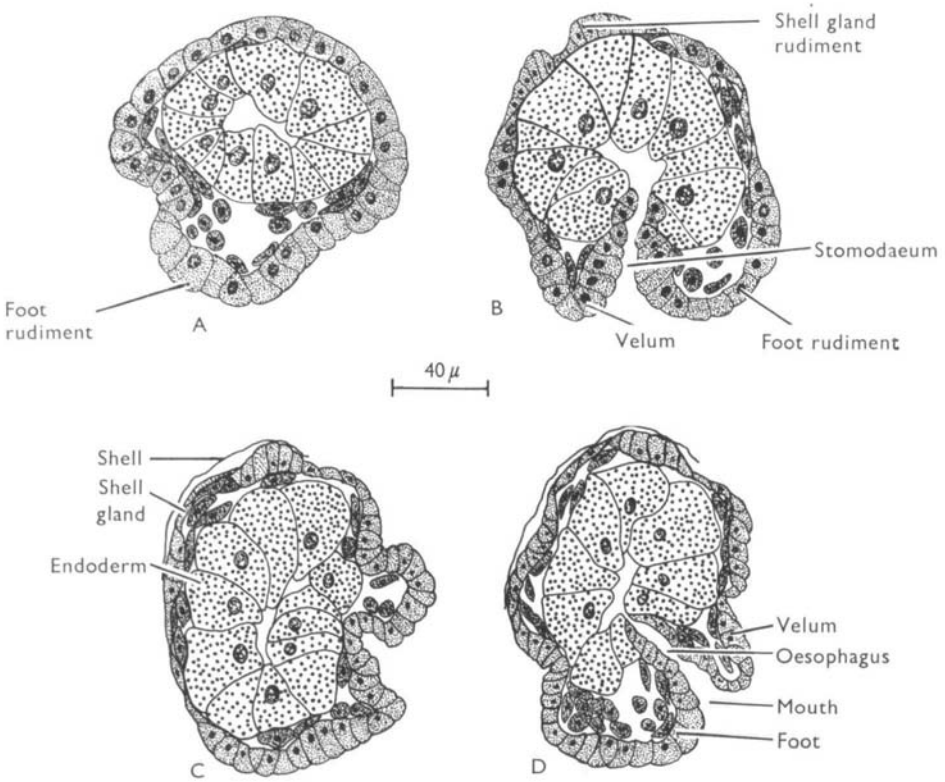

Text-fig. 4. A, Oblique longitudinal section through the early trochophore (70 h); B, median longitudinal section through the late trochophore (100 h); C, median longitudinal section through the early veliger (110 h); D, median longitudinal section through the early veliger (115 h).

The anterior part of the blastopore remains open and its lips give rise to the stomodaeal invagination (Text-fig. 4B), lined by columnar ectodermal cells and opening posteriorly into the archenteron. The latter is walled by large yolk-filled, endoderm cells (Text-fig. 4D).

During the differentiation of the ectodermal structures of the trochophore, the nucleus of each cell remains strongly positive for DNA and becomes more strongly positive for alkaline phosphatase. At the same time, the nucleolar and cytoplasmic RNA in each cell is much increased. A similar pattern is displayed in the mesoderm cells. High iron, alkaline phosphatase, PAS-positive material and glycogen concentrations in the cytoplasm are restricted to the endoderm cells (Table 6).

The veliger. The trochophore transforms gradually into the veliger (Text-fig. 7).

The ectoderm cells of the foot (Text-figs. 4D, 5E) become ciliated, cells in the midline of the foot developing especially long cilia, which beat towards the mouth. Statocyst rudiments, two lateral inward proliferations of the foot epithelium, develop near the junction of the foot and head. As the veliger develops further, they are pinched off internally as solid spheres (Text-fig. 5D). A lumen appears in each and enlarges, and the cells of the wall become flattened and secrete the statolith (Text-fig. 6).

Table 6. *Cytochemical localizations in the trochophore*

Stage	Results of cytochemical tests					
	DNA	RNA	Alkaline phosphatase	Iron	PAS-positive	Glycogen
Trochophore						
Foot cells						
Nucleus	++	−	++	−	−	−
Nucleolus	−	++	++	−	−	−
Cytoplasm	−	++	+	+	+	+
Shell gland cells						
Nucleus	++	−	++	−	−	−
Nucleolus	−	++	++	−	−	−
Cytoplasm	−	++	+	+	+	+
Prototroch cells						
Nucleus	++	−	+	−	−	−
Nucleolus	−	++	+	−	−	−
Cytoplasm	−	++	+	+	+	+
General ectoderm	++	++	+	−	−	−
Endoderm						
Nucleus	+	−	−	−	−	−
Nucleolus	−	+	+	+	+	+
Cytoplasm	−	+	++	++	++	++
Mesoderm	++	++	+	−	−	+

Notation as for Table 3.

Lateral outgrowths of the prototroch, in the form of two ciliated lobes of high columnar cells, become the velum (Text-fig. 5F). The margin of the velum is strongly ciliated, grooved and pigmented (Text-fig. 7). In the prevelar area, a ciliated apical plate organ (Text-fig. 7), composed of several vacuolated cells, develops in a median position, and an eye develops from a group of pigmented epithelial cells on each side.

In the visceral mass, the ectoderm cells at the periphery of the shell gland remain as high columnar cells, while those in the central region of the gland flatten (Text-fig. 5C). The periphery grows as the mantle fold (Text-figs. 5E, 6)

and at the same time, the shell becomes more extensive. Pigmentation and coiling of the shell begin about the seventh day of development.

The rudiments of the nervous system (Text-figs. 5E, 6) arise as proliferations of the ectoderm. The visceral ganglion develops in the anterior mantle region,

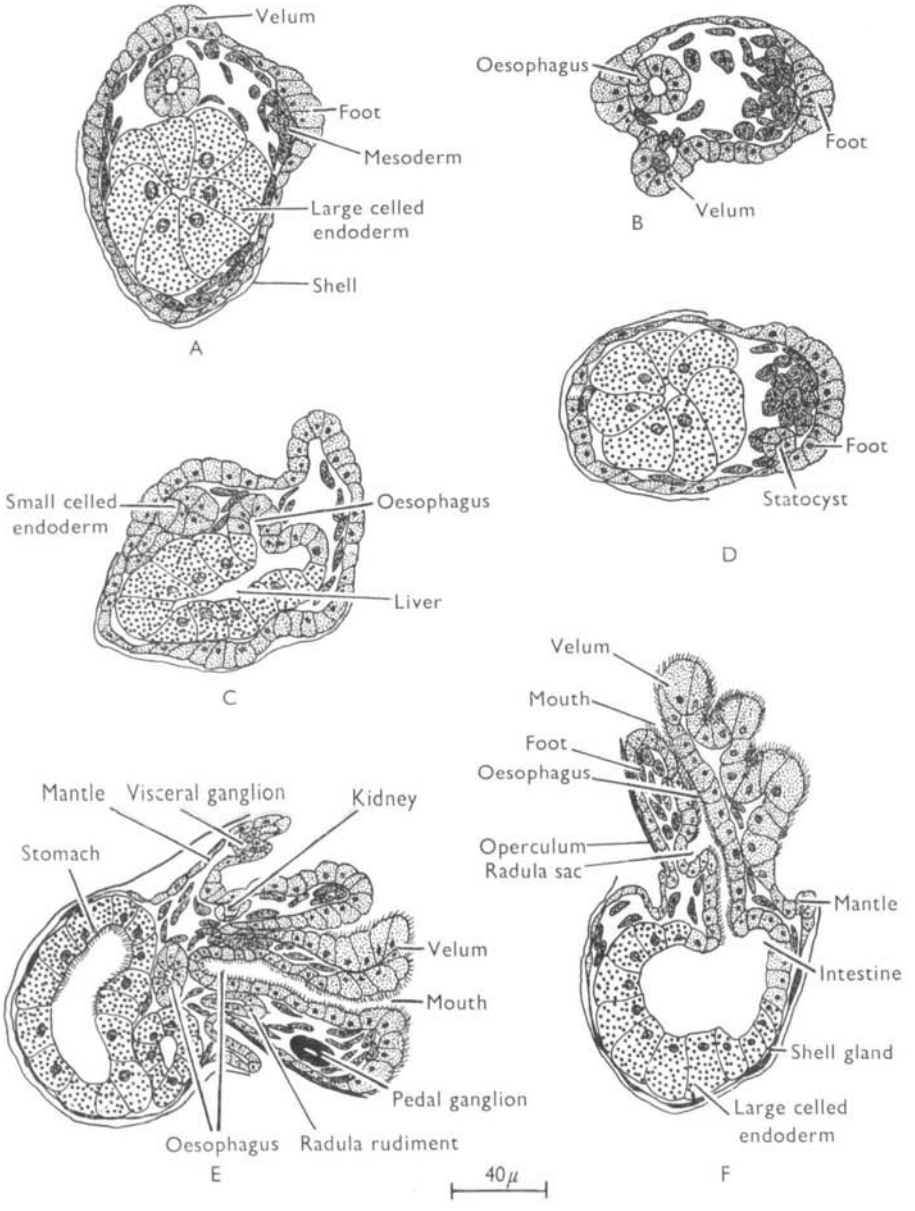

Text-fig. 5. A, Longitudinal section through the early veliger (118 h); B, transverse section through the early veliger (118 h); C, transverse section through the veliger at the beginning of torsion (120 h); D, oblique longitudinal section through the veliger (120 h); E, longitudinal section through the later veliger (180 h); F, longitudinal section through the veliger (150 h).

the cerebral ganglia in the prevelar region, the buccal ganglia by posterior proliferation of the cerebral ganglia, the pedal ganglia in the antero-lateral ectoderm of the foot and the pleural ganglia in the neck region behind the velum.

The larval heart (Text-fig. 7) develops as a vesicle from a solid mass of ectoderm cells to one side of the small-celled endoderm of the hind gut. It begins beating about 10 days after oviposition of the eggs. The larval kidneys found at the base of the velum each comprise three large cells filled with brown vacuoles.

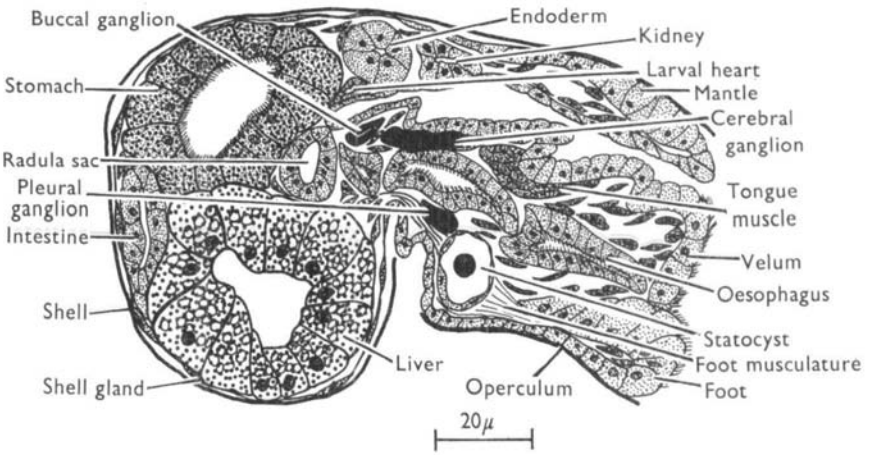

Text-fig. 6. Longitudinal section through the late veliger, just prior to hatching (380 h).

The stomodaeal funnel elongates to give rise to the oesophagus (Text-fig. 5B, F), which opens into the lumen of the archenteron. The radula rudiment (Text-fig. 5F) buds out from the posterior wall of the stomodaeum. The cells of the oesophagus become ciliated, the ventro-median cells, which are continuous with the median ciliated cells of the foot, bearing especially long cilia.

Certain trends common to all ectodermal rudiments can be observed in cytochemical localizations during development of the veliger (Table 7). During the early differentiation of the ectodermal rudiments in the trochophore, each cell exhibits a marked positive reaction for DNA and alkaline phosphatase in the nucleus, while the nucleolar and cytoplasmic RNA are increased. In the veliger, in the ectoderm cells of those organs which, while still differentiating through to the adult type, become functional in the larva, e.g. foot, shell gland, mantle fold and nervous system, the original pattern persists. However, in the cells of those rudiments forming functional temporary larval organs involved in locomotion and nutrition, e.g. the ciliated and pigmented marginal velar cells, the median ciliated cells of the stomodaeum, oesophagus and foot, and the eye, statocysts, larval heart and larval kidneys, the DNA, RNA and nuclear alkaline phosphatase rapidly decrease and these substances may eventually be no longer detectable. In some cells, e.g. the median ciliated cells of the foot, stomodaeum and oeso-

phagus and the statocyst cells, alkaline phosphatase persists in large amounts in the cytoplasm, chiefly in the form of granules. All of the larval cells in the late veliger gain large amounts of PAS-positive material and glycogen.

The endoderm (Text-fig. 4D) in the early veliger is composed of a few large, vacuolated, yolk-filled cells. These later become differentiated into small, rapidly dividing cells and large yolky cells containing albumen vacuoles. The small-celled endoderm first becomes obvious in the anterior and ventral parts of the archenteron wall at the beginning of torsion (Text-fig. 5C). Its cells give rise to the stomach and intestine (Text-fig. 5E, F) and later, by a posterior outgrowth, to the endoderm of the hind gut (Text-fig. 6). The cells of the stomach become large and ciliated and contain many granules. The large-celled endoderm gives rise to a single larval digestive gland (Text-figs. 6, 7). The cells of this organ are large and yolky in the early veliger and, in the later veliger, become filled with albumen vacuoles.

Table 7. *Cytochemical localizations in the veliger*

Stage	Results of cytochemical tests					
	DNA	RNA	Alkaline phosphatase	Iron	PAS-positive	Glycogen
Veliger. Larval organs: large ciliated cells of:						
Foot	+	+	++	++	++	++
Stomodaeum	+	+	++	++	++	++
Oesophagus	+	+	++	++	++	++
Velum	+	−	++	++	++	++
Apical organ	+	−	++	++	++	++
Larval kidney cells	−	−	+	++	+	+
Larval heart cells	+	+	+	+	+	+
Statocyst cells	++	+	++	+	−	−
Larval liver cells	+	−	++	++	++	++
Ectodermal adult rudiments	++	++	+	−	−	−
Endodermal adult rudiments	++	++	+	+	+	+
Mesodermal adult rudiments	++	++	+	−	−	+

Notation as for Table 3.

The cytochemical composition of the endoderm cells (Table 7) is dominated by the presence of yolk during early embryogenesis, and all cells have therefore a high alkaline phosphatase, iron, PAS-positive material and glycogen content. With the onset of differentiation of the small-celled endoderm reactions for nuclear DNA and alkaline phosphatase and nucleolar and cytoplasmic RNA become more positive in these cells. At the same time, the amount of glycogen, PAS-positive material and iron decreases, although a border rich in alkaline phosphatase persists in the cells of the stomach.

Prior to the utilization of yolk in the large-celled endoderm cells of the larval

liver, cytochemical localizations are typical of yolk-filled cells. With utilization of the yolk, the larval liver cells retain reduced but appreciable amounts of iron, glycogen, PAS-positive material and alkaline phosphatase. In the fully differentiated cells of the larval liver, reactions for nuclear alkaline phosphatase and DNA are only slightly positive, and no nucleolar or cytoplasmic RNA is detectable.

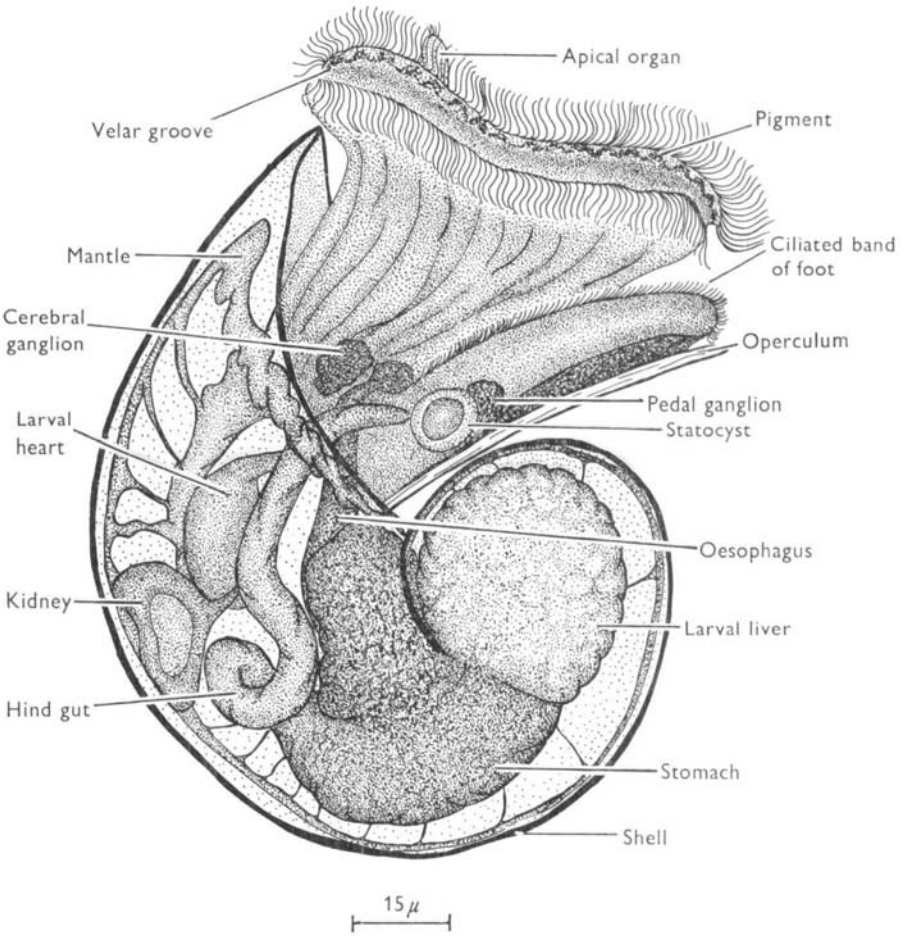

Text-fig. 7. Late veliger, viewed from the right (380 h).

As in the trochophore, ectodermal outgrowths are accompanied in the veliger by proliferations of the mesoderm. The rudiments of the adult kidney and heart first appear as a solid mass of mesoderm tissue near the small-celled endoderm of the hind gut (Text-fig. 6). In the later veliger, the kidney (Text-fig. 7) has a definite cavity and is lined by large cuboidal cells.

Like the other adult rudiment cells, the mesoderm cells are strongly positive for RNA and DNA. They also contain small amounts of alkaline phosphatase and glycogen (Table 7).

DISCUSSION

The embryonic development of *B. nanum* resembles that of *Littorina obtusa* as described by Delsman (1914), but in the veliger a number of differences related to the veliger mode of life can be observed. In *L. obtusa*, the foot rudiment is paired and possesses pedal glands in the late veliger, while that of *B. nanum* is single and possesses no pedal glands. In *L. obtusa*, the velum is simple and the tentacles well developed, but in *B. nanum* the velum is elaborate and the tentacles are not yet developed. The embryo of *L. obtusa* hatches at the crawling stage (Pelseneer, 1911; Delsman, 1914; Thorson, 1946), whereas that of *B. nanum* hatches as a pelagic, planktotrophic veliger (Anderson, 1961).

Little work has been done on cytochemistry of oogenesis and development in littorinids (Raven, 1958, 1961), and the electron microscope has not previously been employed in investigating oogenesis in primitive prosobranch gastropods of this type.

A number of workers (Gall, 1952, 1954; Ris, 1954, 1962; Lafontaine & Ris, 1958; Wolfe, 1965), using phase-contrast and electron microscopy, have attempted to clarify the fine structure of the lampbrush chromosome. As far as can be judged from the present material, the structure of the loop in *B. nanum* appears to be a helically coiled bundle of submicroscopic fibres. As in other molluscan oocytes (Raven, 1958; Hess, 1962), DNA can be demonstrated by the Feulgen technique only in the early germinal vesicle of *B. nanum*, not in the late germinal vesicles, in which the lampbrush chromosomes are well dispersed.

In *B. nanum*, no highly organized structural components were found in the oocyte nucleoli, the nucleoli being composed of amorphous, electron dense, granular material similar to the pars amorpha described by Estable & Sotelo (1954) in rat oocyte nucleoli. Many modes of transfer of nucleolar material to the cytoplasm in developing oocytes have been postulated (Raven, 1961; Feldherr, 1964). In the oocytes of *B. nanum*, the granulated membraneous pouches, which cover the annuli of the nuclear membrane, may be sites of transfer of material released from the nucleoli and accumulated under the nuclear membrane. In the early oocyte, when cytoplasmic synthesis is high, these pouches project into the cytoplasm; but later, when yolk is being deposited, they project into the nucleoplasm. It has been well established (Porter, 1961) that in cells with high protein synthesis, the nucleoli are large and have a high RNA content. The high RNA, alkaline phosphatase and PAS-positive material content and the changes in amount and distribution of nucleolar material in the developing oocytes of *B. nanum* are indicative of the intense metabolic activity of this organelle, associated with a variety of cytoplasmic syntheses prior to yolk deposition.

As in other oocytes (Raven, 1961), the early phase of oocyte growth involves cytoplasmic increase, and this is then followed by deposition of yolk. These two phases will be discussed separately.

In *B. nanum*, prior to vitellogenesis and after an early undifferentiated stage,

an endoplasmic reticulum is developed which approaches in complexity that of protein-synthesizing somatic cells (see Porter, 1961). During elaboration of the endoplasmic reticulum, mitochondria and Golgi bodies also increase in number and disperse throughout the cytoplasm. The increasing complexity of the endoplasmic reticulum in both the parallel granulated lamellae and in the vitelline body, and the subsequent decrease in significance of these organelles during vitellogenesis, is accompanied by a parallel increase, followed by decrease in RNA, alkaline phosphatase and iron. These observations point to the endoplasmic reticulum as a site of synthesis in the cytoplasm of the oocytes of *B. nanum*.

Fatty yolk formation. Raven (1961) reviewed the possible modes of fatty yolk formation. While fatty yolk appears in association with mitochondria in the vitelline body and in other parts of the cytoplasm in *B. nanum*, no accumulation of lipid material within mitochondria or transformation of mitochondria into lipid droplets, as suggested by Ward (1962) in *Rana* oocytes, was observed in *B. nanum*. Because of the role played by mitochondria in energy production and transfer, and the increase in size and number of the mitochondria, prior to vitellogenesis and decrease following the commencement of yolk deposition, the mitochondria in *B. nanum* oocytes presumably play some part in synthesis of fatty yolk, but their precise role is not yet clear.

Proteid yolk formation. Proteid yolk formation has often been reported in association with the Golgi apparatus (Bretschneider & Raven, 1951; Bolognari, 1960*a*, *b*; Worley & Hershenov, 1960). In the oocytes of *B. nanum*, the proteid yolk is deposited in swollen Golgi vesicles and, in the mature oocyte, the platelets are surrounded by membraneous fragments of the Golgi vesicles. From the above information, it can be inferred that the Golgi apparatus plays some part in condensation and modification, if not synthesis, of proteid yolk in this species.

Accompanying the synthesis of yolk in the oocyte of *B. nanum*, there is an increase in PAS-positive material, glycogen, iron and alkaline phosphatase associated with the yolk. This implies an increase in the amount of energy yielding and constructive materials, accompanied by an increase in substances possibly involved in their further synthesis, breakdown and transfer, although the source of these substances is still obscure.

At the end of oogenesis in other molluscan oocytes, neither specific localizations of ultra-structural organelles (Raven, 1958, 1961; Hess, 1962; Pasteels & de Harven, 1963) nor definite localizations of cytochemically detectable material (Raven, 1961; Hess, 1962) have been recorded. A similar absence of pattern occurs in the late oocyte of *B. nanum*, where the ultra-structural organelles are found scattered throughout the cytoplasm and no gross preferential cytoplasmic distribution of the materials tested can be observed.

Fertilized egg. Cytochemical localizations in the fertilized egg of *B. nanum* are characterized by slight radial and animal-vegetal gradients, indicating a change with fertilization. Increases in cytoplasmic RNA and alkaline phos-

phatase are indicative of renewed synthetic activity, particularly in the subcortical plasm.

Cleavage. A more definite animal-vegetal cytochemical gradient, associated with yolk distribution, is established during cleavage in *B. nanum*, but it must be stressed that the differences between various cleavage cells are only relative, with no regional localizations occurring in any one cell or group of cells. The increase in total DNA during cleavage in *B. nanum* is accompanied by alkaline phosphatase increase, suggesting high rates of nuclear metabolism. Cytoplasmic localizations point to an amplification of cytoplasmic syntheses, which seem to increase further in the micromeres of later cleavage stages, in which cytoplasmic and nucleolar RNA are high.

Gastrulation. Gastrulation in *B. nanum* is accompanied, as in other molluscs (Raven, 1958; Hess, 1962), by progressive histological and cytochemical differentiation of the ectoderm, endoderm and mesoderm. Ectodermal and mesodermal cytochemical localizations reflect the increased synthesizing activity in these cells and their resulting increased morphogenetic potential. During further embryogenesis, these cells are the actively differentiating cells of the trochophore and veliger. The conspicuous elements of the endodermal localizations may provide a basis for oxidative, degradative and synthetic processes in these cells.

Organogenesis. Early in organogenesis in *B. nanum*, cytochemical localizations reflect the immediate morphogenetic potentials of the cell types. Raven (1946, 1958) found a similar pattern in the embryo of *Limnaea*. Differentiating cells, whether larval or adult, are rich in RNA, DNA and alkaline phosphatase, and poor in iron, glycogen and PAS-positive material. Synthesizing activities are presumably at a maximum in these cells and cytochemical localizations are not yet related to functional differences between the cells.

Following this initial differentiation, two distinct cell types arise: (1) Adult rudiment cells which may be functional, but are still differentiating towards the adult type, e.g. shell gland and mantle fold, nervous system; or are of minor functional importance in the larva, e.g. muscles, adult heart and kidney rudiments. These cells retain a high level of detectable DNA, RNA and alkaline phosphatase. (2) Functional temporary larval cells involved in locomotion and nutrition, e.g. ciliated cells of the velar margin, ventro-median cells of the stomodaeum and oesophagus and larval liver cells. These show reduced detectable DNA, RNA and alkaline phosphatase, but increased PAS-positive material, glycogen and iron content. The less intense Feulgen reactions in the nuclei of these cells may be due to dispersal of nuclear material in the relatively large nuclei or to an actual reduction in DNA content, due to breakdown of DNA in the nuclei of the cells, which are resorbed at the end of larval life. It is doubtful whether the less intense Feulgen reaction is due to a change in ploidy.

SUMMARY

1. Embryonic development in *B. nanum* is similar to that of *Littorina obtusa*, apart from differences, especially in the velum and foot, which can be correlated with the planktonic mode of life of the veliger of *B. nanum*.

2. Electron microscope studies of oogenesis show that fatty yolk formation occurs in association with the vitelline body and with mitochondria, and proteid yolk formation occurs in association with the Golgi apparatus. Nucleo-cytoplasmic relationships in the growing oocyte are discussed.

3. During oogenesis, cytochemical localizations can be related to the nucleolar activity, elaboration of the endoplasmic reticular elements and the presence of yolk. No preferential distribution of the substances tested occurs in the cytoplasm of the late oocyte.

4. Following fertilization, slight animal-vegetal and radial gradients are established, chiefly in association with the yolk.

5. During cleavage, a definite animal-vegetal gradient is seen in the pattern of cytochemical localizations, but the differences between the cells are only relative, no rigid localizations in one cell or group of cells occurring.

6. During gastrulation, the chemo-differentiation detectable in early embryonic development is well established. The cells of the ectoderm, endoderm and mesoderm are each cytochemically distinct, but no absolute distinctions between each cell type can be shown.

7. During organogenesis, the initial differentiation of both larval and adult cells is accompanied by strongly positive reactions for DNA, RNA and alkaline phosphatase in these cells. Following this initial differentiation, two distinct cell types emerge:

(i) Functional larval cells (both ectodermal and endodermal) involved in nutrition and locomotion, showing slight reactions for RNA, DNA and alkaline phosphatase (except where these are involved in cell function) and highly positive reactions for iron, glycogen and PAS-positive material.

(ii) Adult rudiment cells, which may be functional in the larva, but are still differentiating towards the adult type and remain strongly positive for DNA, RNA and alkaline phosphatase.

RÉSUMÉ

Microscopie électronique et cytochimie de l'oogenèse, et cytochimie du développement embryonnaire, chez le Gastéropode Prosobranche Bembicium nanum *L.*

1. Le développement embryonnaire de *B. nanum* est semblable à celui de *Littorina obtusa*, mises à part des différences, en particulier dans le velum et le pied, qui peuvent être en corrélation avec le mode de vie planctonique de la véligère de *B. nanum*.

2. L'étude de l'oogenèse au microscope électronique montre que la formation du vitellus lipidique se fait en association avec le corps vitellin et les mitochondries, et que la formation du vitellus protéique a lieu en association avec l'appareil de Golgi. On discute les rapports nucléo-cytoplasmiques dans l'oocyte en croissance.

3. Au cours de l'oogenèse, on peut rapporter des localisations cytochimiques à l'activité nucléolaire, à l'élaboration d'éléments du réticulum endoplasmique et à la présence de vitellus. Il n'y a pas de répartition préférentielle des substances recherchées, dans le cytoplasme de l'oocyte avancé.

4. Après la fécondation s'établissent des gradients modérés, animaux-végétatifs et radiaux, surtout en association avec le vitellus.

5. Au cours de la segmentation, on observe un gradient animal-végétatif défini dans la répartition des localisations cytochimiques, mais les différences entre les cellules sont seulement relatives, car il ne s'établit pas de localisations strictes dans une cellule ou un groupe de cellules.

6. Au cours de la gastrulation, la chimio-différenciation décelable au début du développement embryonnaire est bien établie. Les cellules de l'ectoderme, de l'endoderme et du mésoderme sont, pour chaque feuillet, cytochimiquement distinctes mais on ne peut pas établir de distinctions absolues entre chaque type cellulaire.

7. Au cours de l'organogenèse, la différenciation initiale des cellules larvaires et adultes s'accompagne de réactions fortement positives pour l'ADN, l'ARN et la phosphatase alcaline dans ces cellules. A la suite de cette différenciation initiale, deux types cellulaires distincts émergent:

(*a*) Cellules larvaires fonctionnelles (à la fois ectodermiques et endodermiques) impliquées dans la nutrition et la locomotion, montrant des réactions légères pour l'ARN, l'ADN et la phosphatase alcaline (sauf là où ces substances sont impliquées dans le fonctionnement cellulaire) et des réactions fortement positives pour le fer, le glycogène et le matériel APS-positif.

(*b*) Cellules des ébauches adultes, qui peuvent être fonctionnelles chez la larve mais sont encore en cours de différenciation selon le type adulte, et qui restent fortement positives pour l'ADN, l'ARN et la phosphatase alcaline.

ACKNOWLEDGEMENTS

This work was submitted to the University of Sydney as part of a Master of Science Thesis. The author wishes to thank Dr D. T. Anderson for his many helpful criticisms during this investigation and the preparation of the manuscript. She also wishes to thank Mr C. Shorey and other members of the Electron Microscope Unit, University of Sydney, where the electron microscopy was carried out.

REFERENCES

ANDERSON, D. T. (1961). The reproduction and early life history of the gastropod *Bembicium nanum* (Lamarck, 1822) (Fam. Littorinidae). *Proc. Linn. Soc. N.S.W.* **86**, 203–6.

ARVY, L. (1949). Particularités de l'évolution nucléolaire au cours de l'ovogenèse chez *Limnaea stagnalis* L. *C. r. hebd. Séanc. Acad. Sci., Paris*, **228**, 1982–5.

ARVY, L. (1950). Donnés histologiques sur l'ovogenèse chez *Dentalium entale* Deshayes. *Archs. Biol., Paris*, **61**, 187–96.

BOLOGNARI, A. (1960*a*). Yolk formation in oocytes of *Patella coerulea* L. and *Aplysia depilans* L. as observed in the electron microscope. *Nature, Lond.*, **186**, 490–1.

BOLOGNARI, A. (1960*b*). Golgi bodies and zones in molluscan oocytes. *Nature, Lond.*, **186**, 565–6.

BRACHET, J. (1960). *The Biochemistry of Development.* London: Pergamon.

BRETSCHNEIDER, L. H. & RAVEN, C. P. (1951). Structural and topochemical changes in the egg cells of *Limnaea stagnalis* L. during oogenesis. *Archs neerl. Zool.* **10**, 1–31.

COLLIER, J. R. (1960). Localisation of some phosphorous compounds in the egg of *Ilyanassa obsoleta. Exp. Cell. Res.* **21**, 548–55.

COWDEN, R. R. (1961). Cytochemical investigation of oogenesis and development to the swimming larval stage in the chiton, *Chiton tuberculatum. Biol. Bull. mar. biol. Lab., Woods Hole*, **120**, 313–25.

DELSMAN, H. C. (1914). Entwicklungsgeschichte von *Littorina obtusa. Tijdschr. ned. dierk. Vereen.* **13**, 170–340.

ESTABLE, C. L. & SOTELO, J. R. (1954). Behaviour of nucleolonema during mitosis. In *Fine Structure of Cells*, **8**, 170–90. New York: Interscience.

FELDHERR, C. M. (1964). Binding within the nuclear annuli and its possible effect on nucleocytoplasmic exchanges. *J. Cell Biol.* **20**, 188–92.

GALL, J. G. (1952). The lampbrush chromosomes of *Triturus viridescens. Exp. Cell. Res.* (Suppl.), **2**, 95–102.

GALL, J. G. (1954). Lampbrush chromosomes from the oocyte nuclei of the newt. *J. Morph.* **94**, 283–351.

HESS, O. (1962). Entwicklungsphysiologie der Mollusken. *Fortschr. Zool.* **14**, 130–63.

LAFONTAINE, J. G. & RIS, H. (1958). An electron microscope study of lampbrush chromosomes. *J. biophys. biochem. Cytol.* **4**, 99–106.

PANTIN, C. F. A. (1948). *Notes on Microscopical Technique for Zoologists.* Cambridge University Press.

PASTEELS, J. J. & DE HARVEN, E. (1963). Étude au microscope électronique du cytoplasme de l'œuf vierge et fécondé de *Barnea candida. Archs Biol., Paris*, **74**, 415–37.

PEARSE, A. G. E. (1960). *Histochemistry, Theoretical and Applied.* London: Churchill.

PELSENEER, P. (1911). Recherches sur l'embryologie des Gastropodes. *Brux. Mem. Acad. Roy.* (Ser. 2), **6**, 1–167.

PORTER, K. R. (1961). The ground substance; observations from electron microscopy. *The Cell*, **2**, 621–76. Ed. J. Bracet and A. E. Mirsky. New York: Academic Press.

RAVEN, C. P. (1946). The development of the egg of *Limnaea stagnalis* L. from the first cleavage till the trochophore stage, with special reference to its 'chemical embryology'. *Archs néerl. Zool.* **7**, 353–434.

RAVEN, C. P. (1958). *Morphogenesis: The Analysis of Molluscan Development.* London: Pergamon.

RAVEN, C. P. (1961). *Oogenesis: The Storage of Developmental Information.* London: Pergamon.

REBHUN, L. I. (1956*a*). Electron microscopy of basophilic structures of some invertebrate oocytes. I. Periodic lamellae and the nuclear envelope. *J. biophys. biochem. Cytol.* **2**, 93–109.

REBHUN, L. I. (1956*b*). Electron microscopy of basophilic structures of some invertebrate oocytes. II. Fine structure of the yolk nuclei. *J. biophys. biochem. Cytol.* **2**, 159–70.

REBHUN, L. I. (1961). Some electron microscope observations of membranous basophilic elements of invertebrate eggs. *J. Ultrastruct. Res.* **5**, 208–19.

RIS, H. (1954). The submicroscopic structure of chromosomes. *Fine Structure of Cells*, **8**, 121–34. New York: Interscience.

RIS, H. (1962). Interpretation of ultrastructure of the cell nucleus. *The Interpretation of Ultrastructure. Symp. Int. Soc. Cell Biol.* **1**, 69–88.

STEIN, R. S. & GERADE, H. W. (1950). Cytological demonstration of nucleic acids in tissue culture. *Science*, **111**, 256–7.

THORSON, G. (1946). Reproduction and larval development of Danish marine bottom invertebrates. *Meddr. Kommn. Danm. Fisk. og Havunders* (Ser. Plankton), **4**, 1–523.

WARD, R. T. (1962). The origin of protein and fatty yolk in *Rana pipiens*. Electronmicroscopical and cytochemical observations of young and mature oocytes. *J. Cell Biol.* **14**, 309–41.

WOLFE, S. L. (1965). The fine structure of isolated chromosomes. *J. Ultrastruct. Res.* **12**, 104–12.

WORLEY, L. G. & HERSHENOV, B. (1960). Electron microscopy of the elaboration of a protein yolk by the Golgi complex during early development of *Crepidula*. *Anat. Rec.* **138**, 391 (abstract).

(*Manuscript received 5 July 1965*)